Approximate expressions of a SBR for wastewater treatment: Comparison with numeric solutions and application to predict the biomass concentration in real cases

Cintia C. Lobo [a],[*], Nora C. Bertola [a], Edgardo M. Contreras [b]

[a] Centro de Investigación y Desarrollo en Criotecnología de Alimentos (CIDCA), CONICET—Fac. de Cs. Exactas—UNLP, 47 y 116, B1900AJJ La Plata, Argentina
[b] Instituto de Investigaciones en Ciencia y Tecnología de Materiales (INTEMA), CONICET-Mar del Plata, Av. Juan B. Justo 4302, 7600 Mar del Plata, Argentina

ARTICLE INFO

ABSTRACT

Most industrial wastewater treatment systems often operate under transient conditions, causing several operational problems. An effective solution is the use of Sequencing Batch Reactors (SBR). In general, a great number of simulations are necessary to solve SBRs mathematical models in order to evaluate the effect of the operational conditions on the performance of the reactor. In this work, a set of analytical equations that represent the effect of the operational parameters on the performance of a SBR was developed. The obtained equations adequately represent the change of the organic substrate, ammonia, biomass, oxygen and soluble microbial products as a function of time within a single operation cycle of the SBR. The equations also predict the steady-state concentrations as a function of several operational parameters, avoiding the problem of performing a great number of simulations. Based on real SBR data, the biomass growth yield and the decay factor for two synthetic wastewaters were obtained. Using these coefficients, the proposed equations adequately predicted the biomass concentration in real cases.

© 2016 The Institution of Chemical Engineers. Published by Elsevier B.V. All rights reserved.

1. Introduction

Most industrial processes generate wastewaters which are characterized by their variability of flowrate, composition and concentration of organic compounds. As a result, wastewater treatment systems often operate under transient conditions, causing operational problems related with low removal efficiencies and poor settling properties of the sludge (Edwards, 1995). To solve these problems, an effective approach is the use of Sequencing Batch Reactors (SBR). In general, SBR include five well-defined phases: fill, react, settle, draw and idle (Annesini et al., 2014). These phases can be optimized for each particular case. The main advantages of SBR in comparison with other biological treatments are high flexibility, simple running, compact layout, better control of shock loads, possibility of achieving anoxic or anaerobic conditions in the same tank and good oxygen contact with microorganisms and substrates (Tomei et al., 2004; Wang et al., 2014). For these reasons, SBRs have been used for the treatment of domestic wastewaters (Mines and Milton, 1998; Bagheri et al .,2015) and wastewater from many industries, such as dairy (Yahi et al., 2014), olive mill (Chiavola et al., 2014), pharmaceuticals (Lefebvre et al., 2014), tannery (Ganesh et al., 2006), textile (Kapdan and Ozturk, 2005) and phenolic compounds (Tomei et al., 2004).

Mathematical models to be used for the design and operation of SBRs especially under transient conditions are important tools to improve the performance of this process. In general, mathematical models of SBR consist of a biokinetic model and equations that represent the operation of the SBR. The biokinetic model represents the relationship between the rates of substrates consumption and biomass growth. Activated sludge model #1 (ASM1) and its progeny are the most employed models to predict the activated sludge and SBR systems. In the first version, ASM1 was comprised by 13 compounds and 8 processes with 19 parameters, five of which are stoichiometric and the other 14 are kinetic. The last version (ASM3) is comprised by 13 compounds and 12 processes with 21 kinetic parameters and 15 stoichiometric coefficients (Henze et al., 2000). Once the most suitable biokinetic model is selected, these equations are combined with the equations that represent the operation of the SBR (e.g., mass balances for the relevant compounds, for example). In particular, the solids retention time (θ_C) is a key designing parameter for biological wastewater treatment systems. For example, effluent water quality, oxygen demand, biomass concentration and wasted sludge quantity are controlled by θ_C (Kapdan and Ozturk, 2005; Wu et al., 2011). Moreover, several studies demonstrated that biodegradation of toxic compounds is strongly affected by θ_C through the selection of suitable species to degrade these compounds (Kapdan and Ozturk, 2005; Kim et al., 2005).

Due to the intrinsic complexity of SBR models, the use of simulation platforms is mandatory (Pambrun et al., 2008; Mines and Milton, 1998). While some kinetic coefficients and wastewater characteristics may be assumed, others must be evaluated from suitable experiments (Henze et al., 2000). It must be noted that a huge number of simulations are necessary to evaluate the effect of the solids or hydraulic retention time and the operating conditions (aerobic/anaerobic and the duration time of the reaction phase) on the performance of the SBR. For this reason, in this work a set of analytical equations that represent the effect of the operational parameters on the performance of a SBR was obtained. Then, based on real SBR data, these equations were employed to obtain the two model coefficients necessary to represent the biomass concentration in the SBR. The proposed equations were used to simulate the effect of the solids retention time and type of substrate on the biomass concentration of a SBR under transient conditions.

2.   Materials and methods

2.1.   Chemicals and reagents

Phenol (loose crystals, >99%) was obtained from Sigma (St. Lois, MO, USA). All inorganic salts were commercial products of reagent grade from Anedra (San Fernando, Argentina). Dehydrated cheese whey was from Food S.A. (Villa Maipú, Argentina).

2.2.   Activated sludge

Activated sludge used in this study was cultured in laboratory scale (2.5 L) SBRs. In all cases, reactors were operated at an hydraulic retention time (θ_H) of 80 h. Different solids retention time (θ_C) were obtained by direct wastage of appropriate volumes of the mixed liquor three times a week. Because five feeding cycles a week were performed, the average total time of each cycle was $t_T = 33.6$ h. Taking into account

that all other operations (filling, purge, sedimentation, discharge) comprised 2 h, the average length of the reaction phase was $t_R = 31.6$ h. During the reaction phase, aeration was provided at the bottom of the reactor through an air-stone using two air pumps at 2 L min^{-1}; dissolved oxygen (DO) concentration was maintained above 4 mgO$_2$ L^{-1}. With regard to the settling phase, biomass settling was considered ideal, leading to perfect retention of the biomass. In this sense, suspended solids could not be detected in the supernatant after settling phase. Because the settling phase duration (30 min) represented less than 1.5% of the global cycle duration time (t_T), the biomass decay during this phase was considered negligible.

Three SBRs were used in this work:

- SBR-A was fed with a model wastewater with the following composition (Lobo et al., 2013): (NH$_4$)$_2$SO$_4$ 940 mg, K$_2$HPO$_4$ 500 mg and KH$_2$PO$_4$ 250 mg; all components were diluted in 1 L of tap water. Once the reactor was filled, 2500 mg of dehydrated cheese whey (CW) was added to obtain an initial organic substrate concentration (S_{S0}) of 1000 mgCOD L^{-1}.
- SBR-B was fed with model wastewater with phenol (Ph) as the sole carbon-limiting source (Nuhoglu and Yalcin, 2005): (NH$_4$)$_2$SO$_4$ 226 mg L^{-1}, K$_2$HPO$_4$ 500 mg L^{-1}, KH$_2$PO$_4$ 250 mg L^{-1} MgSO$_4$.7H$_2$O 25.2 mg L^{-1}, MnSO$_4$·H$_2$O 2.52 mg L^{-1}, CaCl$_2$ 2 mg L^{-1}, FeCl$_3$ 1.2 mg L^{-1}. An appropriate volume of a concentrated stock solution of phenol was added to obtain an initial concentration of 300 mgPh L^{-1}, which corresponded to $S_{S0} = 714$ mgCOD L^{-1}. pH was adjusted to 7.0 ± 0.05 by adding a few drops of concentrated solutions of NaOH or HCl. The inoculum of this reactor was obtained from SBR-A.
- SBR-C was used to study the effect of alternating the type of the carbon source of the feeding (cheese whey or phenol) on the biomass concentration (X) of the reactor. This study comprised five feeding phases. During Phases I, III and V, SBR-C was fed with the model wastewater of the dairy industry with cheese whey as the carbon source; in these cases $S_{S0} = 1000$ mgCOD L^{-1}. In Phases II and IV, the reactor was fed with a culture medium with 300 mg L^{-1} of phenol as the carbon source. When the reactor was fed with cheese whey (Phases I, III and V) θ_C was 40 d; during the feeding phases with phenol (II and IV), θ_C was increased to 45 days to prevent the biomass washout. In all cases, the hydraulic retention time was 80 h.

Initial biomass concentration (X_0) and soluble chemical oxygen demand (sCOD) were determined at the beginning of the operation cycle in each reactor.

2.3.   Analytical procedures

Total suspended solids (TSS) were used as a measure for the biomass concentration (X) (Lobo et al., 2013). Duplicate biomass measurements were performed; average and maximum relative errors for TSS were 4% and 13%, respectively. Soluble COD (sCOD) was determined as follows: 3 mL of culture samples were centrifuged for 5 min at 13,000 rpm (Eppendorf 5415 C); then COD of the supernatant was determined using a commercial test (Hach Cat. No. 21259). Samples digestion (2 h at 150 °C) was performed in a Hach COD Reactor 45600; a Hach DR 2000 photometer was used for the absorbance determination of the digested samples.

Process		1 X	2 S_S	3 S_{NH}	4 S_O	5 S_P	Rate
Table 1 – Stoichiometric matrix of the used model and process rate expressions.							
				Compound			
1	Growth	1	$-1/Y$	$-i_{N,BM}$	$-\left((1-Y)/Y\right)$		$\mu_m\left(S/\left(K_S+S\right)\right)\left(NH/\left(K_{NH}+NH\right)\right)\left(S_O/\left(K_O+S_O\right)\right)X$
2	Decay	-1		$\left(i_{N,BM}-f_P i_{N,P}\right)$	$-\left(1-f_P\right)$	f_P	$b\,X$

2.4. Modeling the SBR

Each operating cycle of the SBR comprises the following steps: (1) fill the reactor with raw wastewater, (2) reaction under aerobic conditions during a time t_R, (3) purge a volume V_P of the mixed liquor, (4) stop the aeration to allow the sedimentation of the suspended solids, and (5) withdraw a volume V_S of the supernatant (e.g., the treated wastewater). Then, a new cycle begin with the filling of the reactor with a volume $V_P + V_S$ of raw wastewater. If t_T was the total time of one operation cycle, flowrates corresponding to treated wastewater (Q_{WW}) and purge (Q_P) are

$$Q_{WW} = \frac{V_P + V_S}{t_T} \tag{1}$$

$$Q_P = \frac{V_P}{t_T} \tag{2}$$

By definition, the solids retention time (θ_C) is the ratio between the total biomass in the reactor and the amount of biomass leaving the system per unit time (Metcalf and Eddy, 2003). The total amount of biomass in the reactor is the product between the total volume of wastewater in the reactor (V) and the biomass concentration at the end of the reaction phase (X_F). Because the purge is performed under mixing conditions, the biomass concentration in the wastage stream is X_F. Taking into account Eqs. (1) and (2) and assuming a complete settling of the solids, hydraulic (θ_H) and solids (θ_C) retention time can be expressed as follows

$$\theta_H = \frac{V}{Q_{WW}} = \left(\frac{V}{V_P + V_S}\right)t_T \tag{3}$$

$$\theta_C = \frac{V X_F}{Q_P X_F} = \left(\frac{V}{V_P}\right)t_T \tag{4}$$

According to the definitions of θ_H and θ_C, the initial concentration corresponding to biomass and soluble compounds for a given cycle $i+1$ ($X_{0(i+1)}$, $S_{0(i+1)}$) are related to their final concentrations corresponding to the previous cycle i ($X_{F(i)}$, $S_{F(i)}$) as follows:

$$X_{0(i+1)} = \left(\frac{V-V_P}{V}\right)X_{F(i)} + \left(\frac{V_P+V_S}{V}\right)X_{WW}$$

$$= \left(1 - \frac{t_T}{\theta_C}\right)X_{F(i)} + \frac{t_T}{\theta_H}X_{WW} \tag{5}$$

$$S_{0(i+1)} = \left(\frac{V-V_P-V_S}{V}\right)S_{F(i)} + \left(\frac{V_P+V_S}{V}\right)S_{WW}$$

$$= \left(1 - \frac{t_T}{\theta_H}\right)S_{F(i)} + \frac{t_T}{\theta_H}S_{WW} \tag{6}$$

where X_{WW} and S_{WW} represent the concentration in the influent of biomass and a soluble compound wastewater, respectively. It must be pointed out that in most cases the raw wastewater suffers a pretreatment (e.g., primary

Table 2 – Coefficients of the biokinetic model.			
Coefficient	Units	Value	Reference
μ_m	h^{-1}	0.08	Ramdani et al. (2012)
Y	mgCOD mgCOD^{-1}	0.53	Ramdani et al. (2012)
K_S	mgCOD L^{-1}	2	Ramdani et al. (2012)
K_{NH}	mgN L^{-1}	0.01	Ramdani et al (2012)
K_O	mgO$_2$ L^{-1}	0.2	Ramdani et al. (2012)
b	h^{-1}	0.008	Ramdani et al. (2012)
$i_{N,BM}$	mgN mgCOD^{-1}	0.070	Ramdani et al. (2012)
$i_{N,P}$	mgN mgCOD^{-1}	0.045	Contreras et al. (2011)
f_P	mgCOD mgCOD^{-1}	0.133	Contreras et al. (2011)

sedimentation) that reduce the inlet biomass concentration. For this reason, the biomass concentration of the influent wastewater is negligible ($X_{WW} \cong 0$) in comparison with the biomass in the reactor.

To represent the growth of biomass (X), consumption of organic substrate (S_S), nitrogen source (S_{NH}), oxygen (S_O) and the formation of soluble microbial products (S_P) during the reaction phase, a reduced version of the ASM1 is used (Contreras et al., 2011). Table 1 shows the stoichiometric matrix of the biokinetic model and the expressions corresponding to each process rate. Table 2 shows an example of kinetic and stoichiometric parameters taken from literature used in the simulations to verify the suitability of the obtained analytical expressions. In this work it was assumed that the length of the filling step is negligible in comparison with the extent of the reaction step (t_R) or with the total cycle time (t_T). Thus, for a given operation cycle i, mass balances corresponding to X, S_S, S_{NH}, S_P and S_O during the reaction phase are the following:

$$\frac{dX_{(i)}}{dt} = (\mu - b)\,X_{(i)} \tag{7}$$

$$\frac{dS_{S(i)}}{dt} = -\frac{\mu}{Y}X_{(i)} \tag{8}$$

$$\frac{dS_{NH(i)}}{dt} = \left[-i_{N,BM}\mu + \left(i_{N,BM} - f_P i_{N,P}\right)b\right]X_{(i)} \tag{9}$$

$$\frac{dS_{P(i)}}{dt} = f_P b X_{(i)} \tag{10}$$

$$\frac{dS_{O(i)}}{dt} = k_L a\left(S_{Osat} - S_{O(i)}\right) - \left[\left(\frac{1-Y}{Y}\right)\mu + (1-f_P)b\right]X_{(i)} \tag{11}$$

where $k_L a$ and S_{Osat} are the volumetric mass transfer coefficient for oxygen and the saturation dissolved oxygen concentration during the reaction phase, respectively. To simulate the periodic operation of the SBR, Eqs. (5)–(11) were solved numerically using a fourth order Runge–Kutta algorithm implemented in Sigma Plot 9.0.

3.   Results and discussion

3.1.   *Approximate expressions for a single batch*

Fig. 1 shows an example of the simulation of the time course of X, S_S, S_{NH} and S_P corresponding to a SBR that is periodically operated at $\theta_C = 20$ d and $\theta_H = 80$ h. As a result of the filling step, concentrations of biomass, organic substrate and nitrogen source at the beginning of the reaction phase of a given operating cycle i are $X_{0(i)}$, $S_{S0(i)}$, and $S_{NH0(i)}$, respectively. Then, due to the biomass growth, substrates are consumed. Fig. 1 shows that at a critical time ($t_{C(i)}$) the biomass growth is limited by the absence of the organic substrate ($S_S = 0$). At this point, the biomass concentration reaches its maximum value ($X_{C(i)}$) whereas the ammonia nitrogen concentration is a minimum ($S_{NHC(i)}$) within the cycle. Due to the endogenous decay process, $X_{(i)}$ decrease and $S_{NH(i)}$ and $S_{P(i)}$ increase up to their final values $X_{F(i)}$, $S_{NHF(i)}$, $S_{P(i)}$ at the end of the reaction phase ($t = t_R$). Then, a volume V_P is purged and the sedimentation phase is begun. After the settling step, a volume V_S of the supernatant (e.g., the treated wastewater) is withdrawn and the reactor is ready for the next operation cycle. In the present model it is assumed that biological processes are strictly aerobic. Due to the anaerobic conditions employed during the sedimentation step, the consumption of substrates during this step is negligible. For this reason, $S_{S(i)}$ and $S_{NH(i)}$ concentrations of the outlet stream are equal to their concentrations at the end of the reaction phase. Additionally, because a perfect sedimentation was assumed, the biomass concentration in the outlet stream is zero.

To obtain the concentration profiles depicted in Fig. 1, 50 consecutive operation cycles were simulated. Fig. SD1 shows that initial concentrations of X, S_{NH} and S_P tend to constant values as a function of the cycle number. Thus, results in Fig. 1 represent the steady-state concentration profiles of the SBR.

It must be pointed out that a great number of simulations are necessary to evaluate, for example, the effect of θ_C, θ_H or other operation parameter on the performance of the SBR. For this reason, it would be desirable to find an analytical equation or a set of equations that represent the effect of the operation parameters (e.g., θ_C, θ_H) on the main outputs of the model without performing such amount of simulations.

Although the specific growth rate (μ) is a function of S_S, S_{NH} and S_O (Table 1), under the excess of substrates it can be assumed that $\theta \cong \theta_m$. Conversely, at the critical time (t_C) a given substrate is depleted and $\mu = 0$. Considering these two conditions, the integration of Eq. (7) leads to the following:

$$X_{(i)} = \begin{cases} X_{0(i)}e^{(\mu_m - b)t} & t \le t_{C(i)} \\ X_{C(i)}e^{-b(t - t_{C(i)})} & t > t_{C(i)} \end{cases} \tag{12}$$

where

$$X_{C(i)} = X_{0(i)}e^{(\mu_m - b)t_c} \tag{13}$$

is the biomass concentration at $t = t_{C(i)}$.

In general, most SBRs are designed assuming that the organic substrate is the compound that limits the biomass growth (e.g., $S_{S(i)} = 0$). In this case, combining Eqs. (7), (8) and (12) and solving for $S_{S(i)}$

$$S_{S(i)} = \begin{cases} S_{S0(i)} - \dfrac{1}{Y_{obs}}\left[X_{(i)} - X_{0(i)}\right] & t \le t_{C(i)} \\ 0 & t > t_{C(i)} \end{cases} \tag{14}$$

where

$$Y_{obs} = Y\left(\dfrac{\mu_m - b}{\mu_m}\right) \tag{15}$$
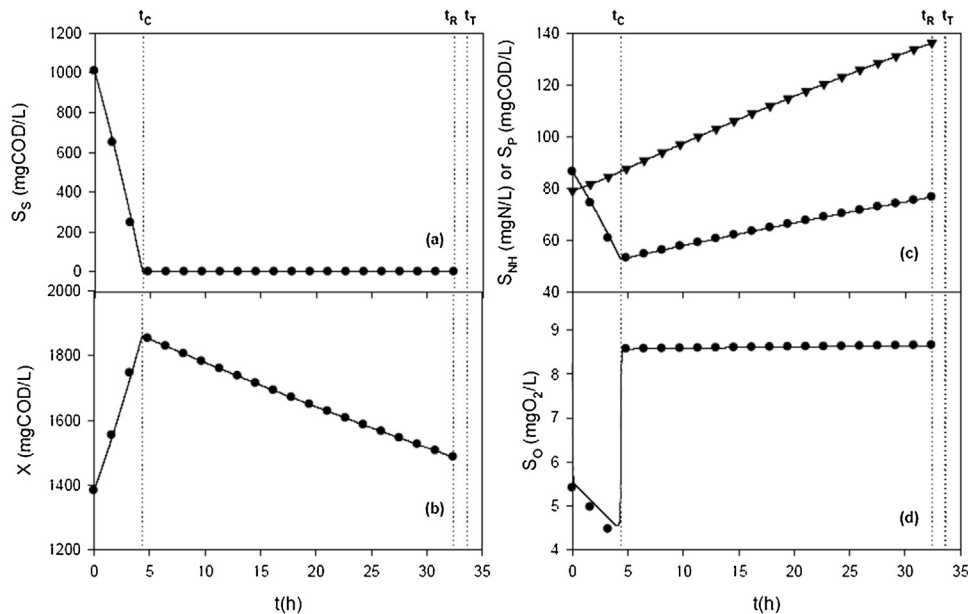

Fig. 1 – Concentration profiles of (a) organic substrate (S_S), (b) biomass (X_0), (c) microbial products (triangles, S_P), ammonia nitrogen (circles, S_{NH}), and (d) dissolved oxygen (S_O) as a function of the reaction time corresponding to a SBR under steady-state conditions. Continuous lines represent the results obtained by numerical integration of the used model (Tables 1 and 2). Dotted lines indicate the critical (t_C), reaction (t_R) and total time (t_T) of the cycle. Symbols represent the results obtained using Eqs. (12)–(26). Initial conditions (X_0, S_{S0}, S_{NH0}) were adopted from the cycle #50 of Fig. SD1. Simulation conditions: $\theta_H = 80$ h, $\theta_C = 20$ d, $t_R = 32.4$, $t_T = 33.6$ h, $S_{SWW} = 2400$ mgCOD L^{-1}, $S_{NHWW} = 100$ mgN L^{-1}, $S_{PWW} = 0$, $X_{WW} = 0$, $k_L a = 30$ h^{-1}, $S_{Osat} = 9$ mgO$_2$ L^{-1}.

is the observed growth yield. From Eq. (14), the critical biomass concentration can be calculated considering that at $t = t_{C(i)}$, $S_{S(i)} = 0$

$$X_{C(i)} = X_{0(i)} + Y_{obs} S_{S0(i)} \tag{16}$$

It must be noted that $X_{C(i)}$ is the maximum biomass concentration. Then, the critical time can be obtained by combining Eqs. (13) and (16)

$$t_{C(i)} = \frac{1}{(\mu_m - b)} \ln \left(1 + Y_{obs} \frac{S_{S0(i)}}{X_{0(i)}} \right) \tag{17}$$

with regard to the ammonia nitrogen, using a similar procedure the following expression can be obtained

$$S_{NH(i)} = \begin{cases} S_{NH0(i)} - Y_{NG} \left[X_{(i)} - X_{0(i)} \right] & t \le t_{C(i)} \\ S_{NHC(i)} + Y_{ND} \left[X_{C(i)} - X_{(i)} \right] & t > t_{C(i)} \end{cases} \tag{18}$$

where

$$Y_{NG} = \frac{i_{N,BM}\mu_m - (i_{N,BM} - f_P i_{N,P}) b}{\mu_m - b} \tag{19}$$

$$Y_{ND} = i_{N,BM} - f_P i_{N,P} \tag{20}$$

$$S_{NHC(i)} = S_{NH0(i)} - Y_{NG} \left[X_{C(i)} - X_{0(i)} \right] \tag{21}$$

$S_{NHC(i)}$ is the ammonia nitrogen concentration at $t = t_{C(i)}$, which corresponds to a minimum within the operation cycle i.

The evolution of the soluble product $S_{P(i)}$ as a function of time is as follows:

$$S_{P(i)} = \begin{cases} S_{P0(i)} + f_P \left(\frac{b}{\mu_m - b} \right) \left[X_{(i)} - X_{0(i)} \right] & t \le t_{C(i)} \\ S_{PC(i)} + f_P \left[X_{C(i)} - X_{(i)} \right] & t > t_{C(i)} \end{cases} \tag{22}$$

where

$$S_{PC(i)} = S_{P0(i)} + f_p \left(\frac{b}{\mu_m - b} \right) \left[X_{C(i)} - X_{0(i)} \right] \tag{23}$$

is the soluble product concentration at $t = t_C$. Due to the endogenous decay of the biomass $S_{P(i)}$ is continuously released. Thus, its maximum value is reached at the end of the reaction phase.

The dissolved oxygen concentration (S_O) profile is a function of the biomass and substrates concentrations. In this case, the volumetric mass transfer coefficient ($k_L a$) for oxygen and the saturation dissolved oxygen concentration (S_{Osat}) also affect S_O. To obtain an approximate expression for S_O as a function of time, it was assumed that the derivative term in Eq. (11) is negligible in comparison with oxygen transfer and consumption rates. Under this condition, Eq. (11) leads to the following expression

$$S_{O(i)} = \begin{cases} S_{Osat} - \dfrac{R_{O2T}}{k_L a} & t \le t_{C(i)} \\ S_{Osat} - \dfrac{R_{O2E}}{k_L a} & t > t_{C(i)} \end{cases} \tag{24}$$

where

$$R_{O2T} = \left[\left(\frac{1-Y}{Y} \right) \mu_m + (1 - f_P) b \right] X_{(i)} \tag{25}$$

$$R_{O2E} = (1 - f_P) b X_{(i)} \tag{26}$$

R_{O2T} and R_{O2E} are the total and the endogenous respiration rates, respectively. According to Eq. (24), the minimum dissolved oxygen concentration is reached at $t = t_C$, when $X_{(i)} = X_{C(i)}$ is a maximum.

Fig. 1 shows that concentration profiles of the organic substrate (S_S), biomass (X_0), ammonia nitrogen (S_{NH}), microbial products (S_P) and dissolved oxygen (S_O) obtained by the approximate equations (Eqs. (12)–(26)) are close to those obtained by numerical integration of the biokinetic model (Eqs. (7)–(11)). Eqs. (12)–(26) were also tested under quite different operation conditions; in all cases good agreements with the numerical integration were obtained (see Fig. SD2, for example).

3.2. Calculating the steady-state of a SBR

Eqs. (12)–(26) represent a single batch during the operation of the SBR. For a given batch i, these equations are a function of the microbial kinetic parameters and of the initial concentrations of the variables ($X_{0(i)}$, $S_{S0(i)}$, $S_{NH0(i)}$, $S_{O0(i)}$, $S_{P0(i)}$). If the operation conditions are maintained constants, for a sufficient number of cycles the initial condition of two successive batches tends to be equal (see Fig. SD1, for example). The objective of this section is to obtain the expressions that allow to calculate steady-state concentrations of the SBR as a function of the operation conditions (θ_H, θ_C, t_R, t_T), the wastewater characteristics (S_{SWW}, S_{NHWW}, X_{WW}) and the biokinetic parameters (Table 2).

To obtain Eqs. (12)–(26) (Section 3.1), it was assumed that the soluble organic substrate is depleted within the reaction phase ($S_{SF} = 0$). Therefore, according to Eq. (6) the initial organic substrate concentration (S_{S0}) of the reaction phase is a constant:

$$S_{S0} = \frac{t_T}{\theta_H} S_{SWW} \tag{27}$$

Besides, according to Eq. (12) the biomass concentration (X_F) at the end of the reaction phase ($t = t_R$) is

$$X_F = X_C e^{-b(t_R - t_C)} \tag{28}$$

where X_C is given by Eq. (16). Considering that the biomass concentration of the influent wastewater is negligible ($X_{WW} \cong 0$), combining Eqs. (5), (16) and (28) and solving X_0 under steady-state conditions ($X_{0(i)} = X_{0(i+1)} = X_0$), the following is obtained

$$X_0 = Y_{obs} S_{S0} \left[\frac{(1 - (t_T/\theta_C)) e^{-b(t_R - t_C)}}{1 - (1 - (t_T/\theta_C)) e^{-b(t_R - t_C)}} \right] \tag{29}$$

with regard to S_{NH}, according to Eq. (18) the concentration of the nitrogen source at the end of the reaction phase (S_{NHF}) is

$$S_{NHF} = S_{NH0} - Y_{NG} Y_{obs} S_{S0} + Y_{ND} (X_C - X_F) \tag{30}$$
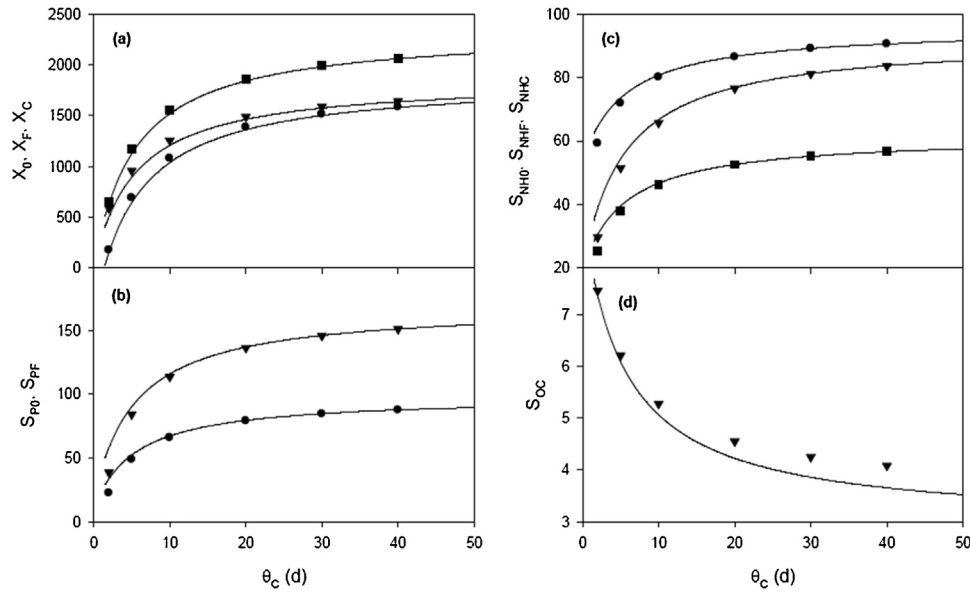
Fig. 2 – Initial (circles), final (squares) and critical (triangles) concentrations as a function of the solids retention time (θ_C) corresponding to a SBR under steady-state conditions: (a) biomass (X), (b) microbial products (S_P), (c) ammonia nitrogen (S_{NH}) and (d) dissolved oxygen (S_O). Dots represent the results by numerical integration of the used model (Tables 1 and 2). Lines indicate the results using Eqs. (27)–(35) assuming $t_C = t_{C\infty}$ (Eq. (37)). Simulation conditions: $\theta_H = 80\,h$, $\theta_C = 20\,d$, $t_R = 32.4$, $t_T = 33.6\,h$, $S_{SWW} = 2400\,mgCOD\,L^{-1}$, $S_{NHWW} = 100\,mgN\,L^{-1}$, $S_{PWW} = 0$, $X_{WW} = 0$, $k_L a = 30\,h^{-1}$, $S_{Osat} = 9\,mgO_2\,L^{-1}$.

In this case, combining Eqs. (6) and (30) and solving for S_{NH0}

$$S_{NH0} = S_{NHWW} - \left(\frac{\theta_H}{t_T} - 1\right)[Y_{NG}Y_{obs}S_{S0} - Y_{ND}(X_C - X_F)] \quad (31)$$

Knowing S_{NH0}, the minimum value of S_{NH} (S_{NHC}) can be obtained as follows

$$S_{NHC} = S_{NH0} - Y_{NG}Y_{obs}S_{S0} \quad (32)$$

with regard to the soluble product (S_P), using a similar procedure the following expression can be obtained

$$S_{PF} = S_{P0} + f_p\left(\frac{b}{\mu_m - b}\right)Y_{obs}S_{S0} + f_p(X_C - X_F) \quad (33)$$

Combining Eqs. (6) and (33)

$$S_{P0} = \left(\frac{\theta_H}{t_T} - 1\right)\left[f_p\left(\frac{b}{\mu_m - b}\right)Y_{obs}S_{S0} + f_p(X_C - X_F)\right] \quad (34)$$

Finally, according to Eq. (26) the minimum dissolved oxygen concentration (S_{OC}) within the reaction phase can be calculated as follows

$$S_{OC} = S_{Osat} - \frac{[((1 - Y)/Y)\mu_m + (1 - f_P)b]}{k_L a}X_C \quad (35)$$

Besides, solving $k_L a$ from Eq. (35), the value of $k_L a$ that required achieving a dissolved oxygen concentration higher than a critical value (S_{OC}) can also be obtained.

Eqs. (27)–(35) represent the steady-state of the SBR. The key issue to employ these equations is to obtain X_0; if X_0 is known then all other equations can be solved. According to Eq. (29), X_0 depends on t_C, which in turn depends on the ratio S_{S0}/X_0 (Eq. (17)). Unfortunately, from the combination of Eqs. (17) and (29), an expression for X_0 that cannot be solved analytically is obtained. To solve this problem, the following approximation is proposed. According to Fig. 1, X_0 increases as

a function of θ_C, tending to an asymptotic value (X_∞). Besides, Eq. (17) demonstrates that if S_0 is constant, t_C decreases as X_0 increases. Because X_∞ is the maximum biomass concentration obtained at very high θ_C values, $t_{C\infty}$ is the minimum critical time that can be achieved. Thus, for $X_0 = X_\infty$ it can be assumed that t_C is negligible in comparison with t_R. Under these conditions Eq. (29) can be simplified as follows

$$X_\infty = \lim_{\theta_C \to \infty}\left(Y_{obs}S_{S0}\left[\frac{(1 - (t_T/\theta_C))\,e^{-b(t_R - t_C)}}{1 - (1 - (t_T/\theta_C))\,e^{-b(t_R - t_C)}}\right]\right)$$
$$\cong Y_{obs}S_{S0}\left[\frac{e^{-bt_R}}{1 - e^{-bt_R}}\right] \quad (36)$$

and combining Eqs. (17) and (36)

$$t_{C\infty} \cong t_R\left(\frac{b}{\mu_m - b}\right) \quad (37)$$

Then, to obtain the steady-state concentrations of the SBR as a function of the solids retention time (θ_C), $t_{C\infty}$ (Eq. (37)) was introduced as a constant in Eqs. (27)–(35). Fig. 2 shows that initial, final and critical concentrations corresponding to biomass (X), organic substrate (S_S), ammonia nitrogen (S_{NH}), microbial products (S_P) and dissolved oxygen (S_O) obtained by this procedure were similar to those obtained by numerical integration of the used model (Eqs. (7)–(11)). It must be pointed out that once S_{S0} and X_0 are obtained (Eqs. (27) and (29), respectively), t_C can be recalculated using Eq. (17). Fig. SD3 shows that the values of t_C obtained by using the proposed method (e.g., using Eqs. (27)–(37) along with Eq. (17)) were close to those obtained by the numerical integration of Eqs. (7)–(11).
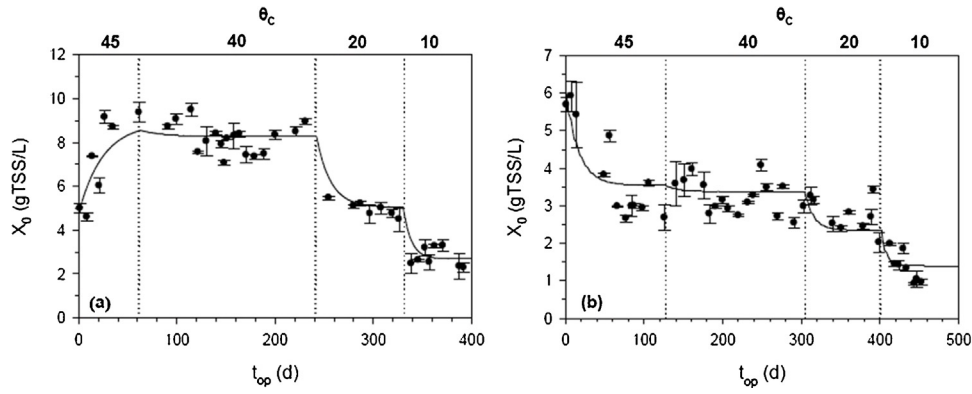
Fig. 3 – Biomass concentration at the beginning of the feeding cycle (X_0) as a function of the operation time (t_{op}) corresponding to (a) SBR-A (feeding with CW) and (b) SBR-B (feeding with Ph). Dotted lines indicate the change of the solids retention time (θ_C). Continuous lines represent the proposed model (Eq. (41)) using the coefficients depicted in Table 3. Dots indicate the average TSS values of duplicates, bars indicate the standard deviation.

3.3. Calculating the observed biomass yield (Y_{obs}) from real SBR data

Fig. 3 shows the evolution of the biomass concentration at the beginning of the reaction phase (X_0) as a function of the operation time (t_{op}) of two SBRs fed with different types of wastewaters. SBR-A was fed with a model wastewater with cheese whey as the carbon source (Fig. 3a); phenol was the sole carbon source in SBR-B (Fig. 3b). Tested θ_C values ranged from 10 to 45 d; in both cases $\theta_H = 80$ h. Fig. 3a shows that within the first 25 days a transient phase was observed in SBR-A. During this phase, X_0 increased up to a constant value of about 9.0 ± 1.0 gTSS L^{-1}. After the transient phase, all reductions of θ_C caused a decrease of X_0.

In the case of SBR-B, Fig. 3b shows that, the initial transient phase lasted about 60 to 70 days. However, in contrast with SBR-A, a decrease of X_0 in SBR-B from 6 to 3 gTSS L^{-1} was observed during the initial transient phase. This difference between both reactors was due to the composition of the feedings. While SBR-A was fed with a complex medium (cheese whey), SBR-B was fed with a mineral medium with phenol as the sole carbon source. Moreover, taking into account the concentrations of cheese whey and phenol of the feeding media and the carbon content per unit mass of cheese whey (0.40 gC gCW^{-1}, (Ferro Orozco et al., 2015) and phenol (0.77 gC gPh^{-1}), SBR-A was fed with a medium that contained about twice the carbon of the medium corresponding to SBR-B. For these reasons, at a given θ_C value the biomass concentration in SBR-A was higher than the corresponding to SBR-B.

Eq. (29) provides a tool to obtain the observed yield (Y_{obs}) from real data of the steady-state biomass concentration in the SBR. Eq. (29) can be rearranged as follows

$$X_0 = \left(\frac{\theta_C - t_T}{\theta_C}\right) X_0 \frac{1}{f_D} - Y_{obs} S_{S0} \tag{38}$$

where

$$f_D = e^{-b(t_R - t_C)} \tag{39}$$

The decay factor (f_D) is the ratio between the final (X_F) and the maximum (X_C) biomass concentration during the reaction phase; f_D depends on t_C, which in turn depends on θ_C. However, if the operating conditions t_R, t_T, S_{S0} are maintained constant, Fig. SD3b shows that for θ_C values higher than 5 d, f_D can be considered as a constant. Thus, the plot of X_0 as a function of $((\theta_C - t_T)/\theta_C) X_0$ would yield a straight line with slope $1/f_D$ and y-intercept $-Y_{obs} S_{S0}$.

Fig. 4 shows that for both SBRs, a linear relationship between X_0 as a function of $((\theta_C - t_T)/\theta_C) X_0$ was obtained. It must be pointed out that biokinetic parameters corresponding to SBR-A and SBR-B are not known, thus, the actual change of f_D as a function of θ_C cannot be calculated (see Fig. SD3b, for example). However, the straight lines obtained in Fig. 4 support the assumption that for both SBRs the change of the decay factor (f_D) was negligible within the tested θ_C values. Using Eq. (38), biomass yields (Y_{obs}) and decay factors (f_D) were obtained (Table 3). Y_{obs} were 0.52 ± 0.02 gTSS gCW^{-1}
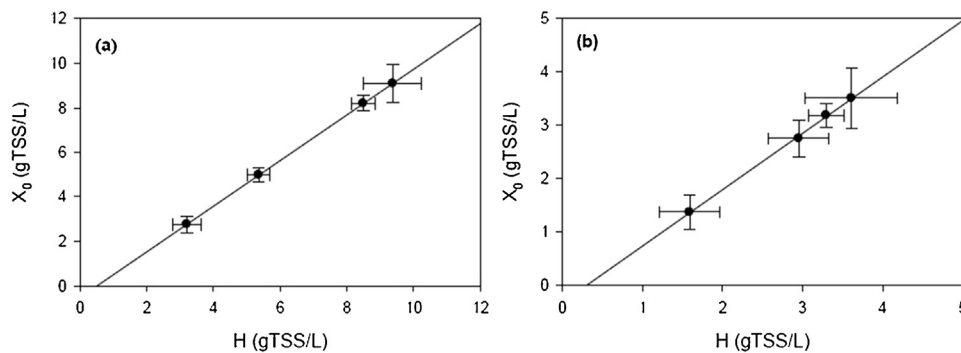

Fig. 4 – Steady-state initial biomass concentration (X_0) as a function of $H = ((\theta_C - t_T)/\theta_C) X_0$. Dots indicate the average value of at least three determinations, bars represent the confidence interval at a level of 95%. Continuous lines represent the linear regression of Eq. (38). Regression results are shown in Table 3.

Table 3 – Observed biomass yield (Y_{obs}) and decay factor (f_D) obtained by linear regression of Eq. (38) to the experimental data corresponding to SBR-A and SBR-B.			
Coefficient	Units	SBR-A (S = CW)	SBR-B (S = Ph)
Y_{obs}	gTSS gS^{-1}	0.52 ± 0.02	1.07 ± 0.25
	gC gC^{-1a}	0.62 ± 0.02	0.66 ± 0.15
	gCOD gCOD^{-1b}	0.67 ± 0.03	0.58 ± 0.14
f_D	–	0.97 ± 0.01	0.95 ± 0.02
r^2		0.9999	0.9988

[a] The following conversion factors were used: carbon content of CW (Ferro Orozco et al., 2015) = 0.40 gC gCW^{-1}, carbon content of Ph (C$_6$H$_6$O) = 0.77 gC gPh^{-1}, carbon content of activated sludge (Ramdani et al., 2012) = 0.53 gC gVSS^{-1}, volatile suspended solids (VSS) to TSS ratio (Ramdani et al., 2012) = 0.90 gVSS gTSS^{-1}.

[b] The following conversion factors were used: chemical demand of oxygen (COD) of CW (Ferro Orozco et al., 2015) = 1.00 gCOD gCW^{-1}, theoretical oxygen demand of Ph = 2.38 gCOD gPh^{-1}, COD of activated sludge (Ramdani et al., 2012) = 1.44 gCOD gVSS^{-1}.
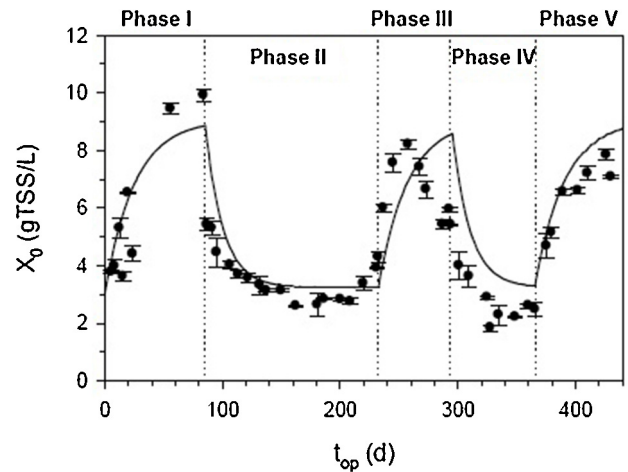

Fig. 5 – Biomass concentration at the beginning of the feeding cycle (X_0) as a function of the operation time (t_{op}). Phases I, III and V, the reactor was fed with CW; Phases II and IV correspond to the feed with Ph. Dotted lines indicate each Phase. Dots indicate the average TSS values of duplicates, bars indicate the standard deviation. Continuous line represents the proposed model (Eq. (41)) using the coefficients depicted in Table 3.

and 1.07 ± 0.25 gTSS gPh^{-1} for SBR-A, and SBR-B, respectively (Fig. 4). Considering the carbon content of both substrates (Ferro Orozco et al., 2015) and of the activated sludge (Ramdani et al., 2012), it can be concluded that in both cases about 60 to 65% of the carbon was transferred from the organic substrate to the biomass (Table 3). Besides, similar results were obtained with regard to the fraction of the electrons of the substrate transferred to the biomass (e.g., Y_{obs} expressed as gCOD gCOD^{-1}). With reference to the term f_D, the following values were obtained: 0.97 ± 0.01 and 0.95 ± 0.02 for SBR-A, and SBR-B, respectively. Taking into account the definition of f_D, it can be concluded that the higher f_D value, the lower endogenous decay coefficient (b). Thus, f_D values indicate that the endogenous decay coefficient for the biomass growing on CW is lower than growing on Ph.

3.4. Dynamics of the biomass concentration in a SBR in response to changes of θ_C

The equations developed in Section 3.1 can be used to calculate the evolution of X_0 as a function of the operation time (t_{op}). According to Eq. (12), the biomass concentration at the end of the reaction phase ($X_{F(i)}$) of a given cycle i is related with the initial biomass concentration ($X_{0(i)}$) as follows

$$X_{F(i)} = \left[X_{0(i)} + Y_{obs} S_{0(i)} \right] f_D \qquad (40)$$

where f_D is the decay coefficient given by Eq. (39). Because it was assumed that the organic substrate is depleted within the reaction phase, $S_{S0(i)}$ only depends on S_{WW} (Eq. (27)). Thus, if S_{WW} is a constant, $S_{S0(i)} = S_{S0(i+1)} = S_{S0}$ is also a constant. Besides, taking into account that the biomass concentration of the influent wastewater is negligible ($X_{WW} \cong 0$), combining Eqs. (5) and (40) the following expression can be obtained

$$X_{0(i+1)} = \left(1 - \frac{t_T}{\theta_C} \right) \left[X_{0(i)} + Y_{obs} S_{S0} \right] f_D \qquad (41)$$

Eq. (41) is composed of two coefficients which are related with the operating conditions (t_T, θ_C), and two biokinetic coefficients (Y_{obs}, f_D). If Y_{obs} and f_D are known (Table 3), from the iteration of Eq. (41) the evolution of $X_{0(i)}$ as a function of

the number of operation cycle (i) can be calculated. Finally, the operation time of the SBR (t_{op}) can be computed as follows

$$t_{op} = t_T (i - 1) \qquad (42)$$

Fig. 3 shows that Eqs. (41) and (42) along with the coefficients depicted in Table 3 adequately describe the dynamics of the biomass concentration at the beginning of the reaction phase (X_0) as a function of the operation time (t_{op}) for both SBR-A and SBR-B.

3.5. Dynamics of the biomass concentration in a SBR in response to changes of the wastewater composition

The effect of the change of the wastewater composition on the biomass concentration was studied in SBR-C. Fig. 5 shows that when SBR-C was fed with the wastewater with cheese whey as the carbon source (Phases I, III and V), an increase of the initial biomass concentration (X_0) was observed. Conversely, when the feeding was changed from cheese whey to phenol (Phases II and IV), a decrease of X_0 was obtained (Fig. 5). This behavior was attributed the difference regarding the carbon content of the complex medium (cheese whey) (Phases I, III and V) in comparison with the mineral medium with phenol as the sole carbon source that was fed in Phases II and IV (see Section 3.3).

Eqs. (41) and (42) along with the coefficients depicted in Table 3 were used to calculate the X_0 in the SBR-C as a function of the operation time (Fig. 5). When the reactor was fed with cheese whey (CW), coefficients corresponding to CW (Table 3) were used in Eq. (41). When the feeding was change from CW to phenol (Ph) it was assumed an instantaneous acclimation of the microorganisms to phenol. According to this assumption, coefficients corresponding to Ph could be used for simulation purposes (Table 3). The authors recognize that this assumption is not strictly correct, particularly during the first days of each change of wastewater. However, the good agreement between experimental and calculated X_0 values (Fig. 5) suggests that the acclimation process of the biomass to phenol

has a negligible effect on the dynamics of the biomass concentration. Thus, in spite of its simplicity, the set of equations developed in the present work can be used to predict the effect of the solids retention time and feeding composition on the biomass concentration in a SBR under transient conditions.

4. Conclusions

In this work a set of analytical equations that represent the effect of several operational parameters on the performance of a SBR was obtained. These equations adequately represent the change of the organic substrate, ammonia, biomass, oxygen and soluble microbial products as a function of time within a single operation cycle of the SBR. Moreover, the obtained equations also predict the steady-state concentrations as a function of several operational parameters, avoiding the problem of performing a great number of simulations. In addition, these equations can be solved using a simple spreadsheet, instead of high cost commercial simulation platforms.

Based on real SBR data, the biomass growth yield and the decay factor for two synthetic wastewaters were obtained. In this work, only two parameters were necessary to predict the dynamic of the biomass concentration in response to the variation on the wastewater characteristics. Thus, the procedure proposed in the present word to predict the biomass concentration is a great simplification in comparison with the use of the ASM3 in a simulation platform. Finally, using the coefficients calculated, the proposed equations adequately represent the change of the biomass concentration in a SBR in response to the variation on the wastewater characteristics.

Acknowledgements

Appendix A. Supplementary data

Supplementary data associated with this article can be found, in the online version, at http://dx.doi.org/10.1016/j.psep.2015.12.008.

References

Annesini, M.C., Piemonte, V., Tomei, M.C., Daugulis, A.J., 2014. Analysis of the performance and criteria for rational design of a sequencing batch reactor for xenobiotic removal. Chem. Eng. J. 235 (0), 167–175, http://dx.doi.org/10.1016/j.cej.2013.09.004.

Bagheri, M., Mirbagheri, S.A., Ehteshami, M., Bagheri, Z., 2015. Modeling of a sequencing batch reactor treating municipal wastewater using multi-layer perceptron and radial basis function artificial neural networks. Process Saf. Environ. 93 (0), 111–123.

Chiavola, A., Farabegoli, G., Antonetti, F., 2014. Biological treatment of olive mill wastewater in a sequencing batch reactor. Biochem. Eng. J. 85, 71–78.

Contreras, E.M., Ferro Orozco, A.M., Zaritzky, N.E., 2011. Biological Cr(VI) removal coupled with biomass growth, biomass decay, and multiple substrate limitation. Water Res. 45 (10), 3034–3046, http://dx.doi.org/10.1016/j.watres.2011.03.011.

Edwards, J.D., 1995. Industrial Wastewater Treatment: A Guidebook. CRC Press, Florida, United States.

Ferro Orozco, A.M., Contreras, E.M., Zaritzky, N.E., 2015. Simultaneous biodegradation of bisphenol A and a biogenic substrate in semi-continuous activated sludge reactors. Biodegradation 26 (3), 183–195.

Ganesh, R., Balaji, G., Ramanujam, R.A., 2006. Biodegradation of tannery wastewater using sequencing batch reactor—respirometric assessment. Bioresour. Technol. 97 (15), 1815–1821, http://dx.doi.org/10.1016/j.biortech.2005.09.003.

Henze, M., Gujer, W., Mino, T., van Loosdrecht, M.C.M., 2000. Activated Sludge Models ASM1, ASM2 ASM2d and ASM3. IWA Scientific and Technical Report No. 9. IWA Publishing, London, UK.

Kapdan, I.K., Ozturk, R., 2005. Effect of operating parameters on color and COD removal performance of SBR: sludge age and initial dyestuff concentration. J. Hazard. Mater. 123 (1–3), 217–222, http://dx.doi.org/10.1016/j.jhazmat.2005.04.013.

Kim, S., Eichhorn, P., Jensen, J.N., Weber, A.S., Aga, D.S., 2005. Removal of antibiotics in wastewater: effect of hydraulic and solid retention times on the fate of tetracycline in the activated sludge process. Environ. Sci. Technol. 39 (15), 5816–5823, http://dx.doi.org/10.1021/es050006u.

Lefebvre, O., Shi, X., Wu, C.H., Ng, H.Y., 2014. Biological treatment of pharmaceutical wastewater from the antibiotics industry. Water Sci. Technol. 69 (4), 855–861.

Lobo, C.C., Bertola, N.C., Contreras, E.M., 2013. Stoichiometry and kinetic of the aerobic oxidation of phenolic compounds by activated sludge. Bioresour. Technol. 136, 58–65.

Metcalf, Eddy, 2003. Wastewater Engineering: Treatment Disposal and Reuse. McGraw Hill, New York, NY.

Mines Jr., R., Milton, G.D., 1998. Bionutrient removal with a sequencing batch reactor. Water Air Soil Pollut. 107 (1–4), 81–89, http://dx.doi.org/10.1023/a:1004948828602.

Nuhoglu, A., Yalcin, B., 2005. Modelling of phenol removal in a batch reactor. Process Biochem. 40 (3–4), 1233–1239.

Pambrun, V., Paul, E., Spérandio, M., 2008. Control and modelling of partial nitrification of effluents with high ammonia concentrations in sequencing batch reactor. Chem. Eng. Process.: Process Intensification 47 (3), 323–329, http://dx.doi.org/10.1016/j.cep.2007.01.028.

Ramdani, A., Dold, P., Gadbois, A., Déléris, S., Houweling, D., Comeau, Y., 2012. Characterization of the heterotrophic biomass and the endogenous residue of activated sludge. Water Res. 46 (3), 653–668, http://dx.doi.org/10.1016/j.watres.2011.11.030.

Tomei, M.C., Annesini, M.C., Bussoletti, S., 2004. 4-Nitrophenol biodegradation in a sequencing batch reactor: kinetic study and effect of filling time. Water Res. 38 (2), 375–384, http://dx.doi.org/10.1016/j.watres.2003.09.023.

Wang, Y.-F., Wang, X.-L., Li, H., Lin, K.-F., Wang, P., Yang, J., et al., 2014. Treatment of high salinity phenol-laden wastewater using a sequencing batch reactor containing halophilic bacterial community. Int. Biodeterior. Biodegrad. 93 (0), 138–144, http://dx.doi.org/10.1016/j.ibiod.2014.04.010.

Wu, C., Peng, Y., Wang, S., Li, X., Wang, R., 2011. Effect of sludge retention time on nitrite accumulation in real-time control biological nitrogen removal sequencing batch reactor. Chin. J. Chem. Eng. 19 (3), 512–517, http://dx.doi.org/10.1016/S1004-9541(11)60014-1.

Yahi, H., Madi, N., Midoune, K., 2014. Contribution to biological treatment of dairy effluent by sequencing batch reactor (SBR). Desalin Water Treat. 52 (10–12), 2315–2321.